

Constraining DGP Gravity from Observational Data

Jun-Qing Xia*

Scuola Internazionale Superiore di Studi Avanzati, Via Beirut 2-4, I-34014 Trieste, Italy

The accelerating expansion of our universe at present could be driven by an unknown energy component (Dark Energy) or a modification of general relativity (Modified Gravity). In this note we revisit the constraints on a phenomenological model which interpolates between the pure Λ CDM model and the Dvali-Gabadadze-Porrati (DGP) braneworld model with an additional parameter α . Combining the cosmic microwave background (CMB), baryon acoustic oscillations (BAO) and type Ia supernovae (SNIa), as well as some high-redshift observations, such as the gamma-ray bursts (GRB) and the measurements of linear growth factors (LGF), we obtain the tight constraint on the parameter $\alpha = 0.254 \pm 0.153$ (68% C.L.), which implies that the flat DGP model is incompatible with the current observations, while the pure Λ CDM model still fits the data very well. Finally, we simulate the future measurements with higher precisions and find that the constraint on α can be improved by a factor two, when compared to the present constraints.

I. INTRODUCTION

Current cosmological observations, such as the CMB measurements of temperature anisotropies and polarization at high redshift $z \sim 1090$ [1] and the redshift-distance measurements of SNIa at $z < 2$ [2], have demonstrated that the universe is now undergoing an accelerated phase of expansion. The simplest explanation is that this behavior is driven by the cosmological constant or the dynamical dark energy models, which suffers from the severe coincidence and fine-tuning problems [3]. On the other hand, this observed late-time acceleration of the expansion on the large scales could also be caused by some modifications of general relativity, such as the scalar-tensor [4] and $f(R)$ theories [5], and gravitational slip [6].

One of the well-known examples is the DGP braneworld model [7], in which the gravity leaks off the four dimensional brane into the five dimensional space-time. On small scales gravity is bound to the four dimensional brane and the general relativity is recovered to a good approximation. In the framework of flat DGP model, the Friedmann equation will be modified as [8]:

$$H^2 - \frac{H}{r_c} = \frac{8\pi G}{3}\rho_m, \quad (1)$$

where $r_c = (H_0(1 - \Omega_m))^{-1}$ is the crossover scale. At early times, $Hr_c \gg 1$, the Friedmann equation of general relativity is recovered, while in the future, $H \rightarrow H_\infty = 1/r_c$, the expansion is asymptotically de Sitter. Recently there have been a lot of interests in the phenomenological studies relevant to the DGP model in the literature [9, 10].

In this note we investigate an interesting phenomenological model, first introduced in Ref.[11], which interpolates between the pure Λ CDM model and the DGP model with an additional parameter α and presents the

tight constraints from the current observations and future measurements. The paper is organized as follows: In Sec. II we describe the general formalism of the modified gravity model. Sec. III contains the current observations we use, and Sec. IV includes our main global fitting results. In Sec. V we present the forecasts from the future measurements, while Sec. VI is dedicated the conclusions.

II. GENERAL FORMALISM

In this phenomenological model, assuming the flatness of our universe, the Friedmann equation is modified as [11]:

$$H^2 - \frac{H^\alpha}{r_c^{2-\alpha}} = \frac{8\pi G}{3}\rho_m, \quad (2)$$

where $r_c = H_0^{-1}/(1 - \Omega_m)^{\alpha-2}$. Thus, we can straightforwardly rewrite the above equation and obtain the expansion rate as following:

$$E^2(z) \equiv \frac{H^2}{H_0^2} = \Omega_m(1+z)^3 + \frac{\delta H^2}{H_0^2}, \quad (3)$$

where the last term denotes the modification of the Friedmann equation of general relativity:

$$\frac{\delta H^2}{H_0^2} \equiv (1 - \Omega_m) \frac{H^\alpha}{H_0^\alpha} = (1 - \Omega_m)E^\alpha(z). \quad (4)$$

Furthermore, we can obtain the effective equation of state:

$$w_{\text{eff}}(z) \equiv -1 + \frac{1}{3} \frac{d \ln \delta H^2}{d \ln(1+z)} = -1 + \frac{\alpha}{3}(1+z) \frac{E'(z)}{E(z)}, \quad (5)$$

where the prime denotes the derivative with respect to the redshift z .

In Fig.1 we illustrate the evolutions of the effective energy density $\Omega_\alpha(z) \equiv 1 - \Omega_m(z)$ and $w_{\text{eff}}(z)$ for different values of parameter α . During the matter dominated era,

*Electronic address: xia@sissa.it

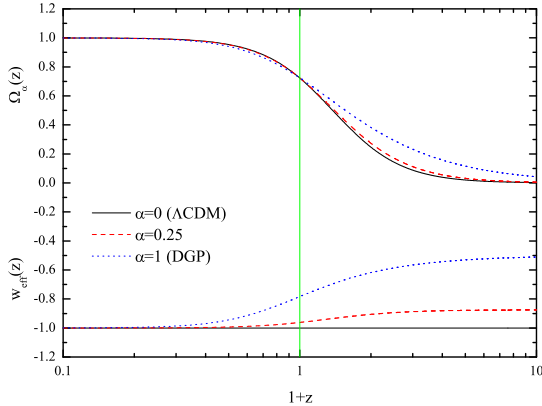


FIG. 1: The evolutions of effective energy density $\Omega_\alpha(z)$ and effective equation of state $w_{\text{eff}}(z)$ for different values of α . The black solid lines are for $\alpha = 0$ (Λ CDM), the red dashed lines for $\alpha = 0.25$ and the blue dotted lines for $\alpha = 1$ (DGP). And the vertical line denotes today ($z = 0$).

$E(z)$ varies as $(1+z)^{3/2}$, which corresponds to the effective equation of state: $w_{\text{eff}} = -1 + \alpha/2$. In the future $z \rightarrow 0$, with the matter density $\rho_m \propto (1+z)^3 \rightarrow 0$, we have $w_{\text{eff}}(z) \rightarrow -1$ and $\Omega_\alpha(z) \rightarrow 1$.

Besides the modification of the Friedmann equation, the flat DGP model also changes the growth function of density perturbation $\delta(a)$. Under assumptions of a quasi-static regime and sub-horizon scales, the correct evolution of perturbation was found [9, 12]:

$$\ddot{\delta} + 2H\dot{\delta} - 4\pi G \left(1 + \frac{1}{3\beta}\right) \rho_m \delta = 0, \quad (6)$$

where the dot denotes the derivative with respect to the cosmic time t , and the β factor is given by:

$$\beta = 1 - 2r_c H \left(1 + \frac{\dot{H}}{3H^2}\right). \quad (7)$$

However, this phenomenological model Eq.(2) is a parametrization, so the situation is more complicated. One of the possible methods was found by Ref.[13]. In order to obtain the growth function of density perturbation within a covariant theory, the authors introduced a correction term and assumed the structure of modified theory of gravity to determine this term. Based on those assumptions, it was consequently found that the β factor was:

$$\beta = 1 - \frac{2}{\alpha} (Hr_c)^{2-\alpha} \left(1 + (2-\alpha) \frac{\dot{H}}{3H^2}\right). \quad (8)$$

In the following analysis, we will use Eq.(6) and Eq.(8) to calculate the growth of density perturbation.

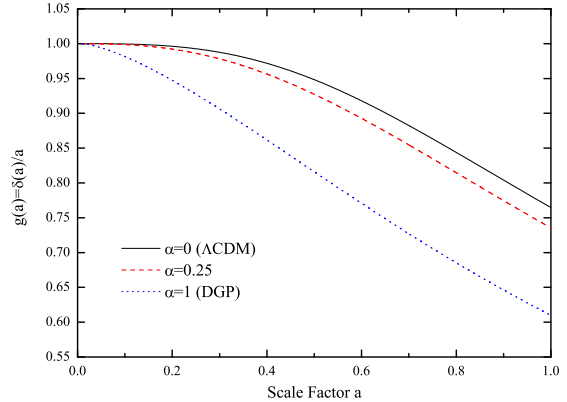


FIG. 2: The evolutions of linear growth $g(a) \equiv \delta(a)/a$ for different values of α . The black solid lines are for $\alpha = 0$ (Λ CDM), the red dashed lines for $\alpha = 0.25$ and the blue dotted lines for $\alpha = 1$ (DGP).

Defined the normalized growth $g(a) \equiv \delta(a)/a$, the growth function Eq.(6) can be rewritten as:

$$\frac{d^2 g}{da^2} + \left(\frac{7}{2} - \frac{3}{2} \frac{w_{\text{eff}}(a)}{1+X(a)}\right) \frac{dg}{ada} + \frac{3}{2} \left[1 - \frac{w_{\text{eff}}(a)}{1+X(a)} - \frac{X(a)}{1+X(a)} \left(1 + \frac{1}{3\beta}\right)\right] \frac{g}{a^2} = 0 \quad (9)$$

where the variable $X(a)$ is the ratio of the matter density to the effective energy density $X(a) = \Omega_m(a)/\Omega_\alpha(a)$. In Fig.2 we plot the linear growth factor $g(a)$ as function of scale factor a for different values of α . One can see that the linear growth factor has been suppressed obviously as long as α is larger than zero. Thus, in the literature the linear growth has been widely used to study the modified gravity models, especially the DGP model [14].

Furthermore, the growth factor can be parameterized as [15]:

$$f \equiv \frac{d \ln \delta}{d \ln a} = \Omega_m^\gamma, \quad (10)$$

where γ is the growth index. And then the growth function becomes:

$$\frac{df}{d \ln a} + \left(\frac{1}{2} - \frac{3}{2} \frac{w_{\text{eff}}(a)}{1+X(a)}\right) f + f^2 - \frac{3}{2} \frac{X(a)}{1+X(a)} \left(1 + \frac{1}{3\beta}\right) = 0. \quad (11)$$

For the pure Λ CDM model, the theoretical value of γ is $6/11 \approx 0.545$, while $\gamma = 11/16 = 0.6875$ in the flat DGP model [16].

In the framework of this phenomenological model, we can easily see that the pure Λ CDM model and flat DGP

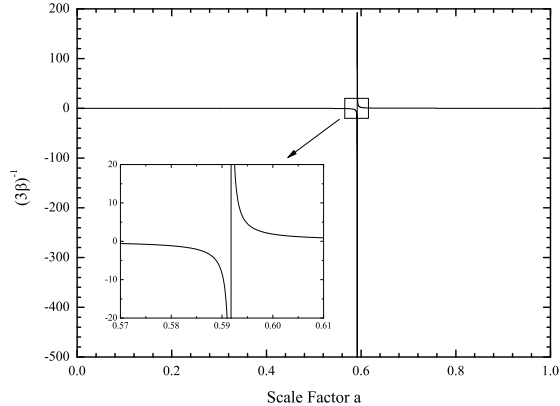


FIG. 3: The evolution of the β term $(3\beta)^{-1}$ when fixing $\alpha = -2$.

model can be recovered when $\alpha = 0$ and $\alpha = 1$, respectively. In order to be consistent with the cosmological observations, the α term should be very small in the early times, such as the Big Bang Nucleosynthesis (BBN) era ($z \sim 10^9$). This limit corresponds to the upper bound: $\alpha < 2$ [11]. On the other hand, when $\alpha < 0$, the effective equation of state will become smaller than -1 , which leads to the instability of linear growth of density perturbation due to the appearance of β term Eq.(8).

At early times, such as the matter dominated era, we have $E(z) \propto (1+z)^{3/2}$ and $\dot{H}/H^2 \simeq -3/2$. Thus, Eq.(8) becomes

$$\beta \simeq 1 - \frac{(\Omega_m(1+z)^3)^{1-\alpha/2}}{1-\Omega_m} \ll 0, \quad (12)$$

since $(1+z)^3 \gg 1$ at $2 < z < 1000$. By contrast, at late times the matter energy density $\rho_m \propto (1+z)^3 \rightarrow 0$ and the expansion is asymptotically de Sitter, $\dot{H} \rightarrow 0$. And then we have

$$\beta \simeq 1 - 2/\alpha \Rightarrow \begin{cases} \beta < 0, & \text{for } 0 < \alpha < 2 \\ \beta > 0, & \text{for } \alpha < 0 \end{cases}. \quad (13)$$

Based on Eq.(12) and Eq.(13), we can straightforwardly see that as long as $\alpha < 0$, during the evolution of universe the value of β should change the sign at one pivot redshift z_t , which leads to $\beta|_{z_t} = 0$ and $(3\beta)^{-1}|_{z_t} \rightarrow \infty$. In Fig.3 we have shown the evolution of $(3\beta)^{-1}$ when fixing $\alpha = -2$. There is an obvious singularity at $a \sim 0.595$. Therefore, based on these discussions above, we use a tophat prior on α as $0 \leq \alpha < 2$ in our calculations.

III. METHOD AND DATA

In our calculations we assume a flat space and use a uniform prior on the present matter density fraction of

the universe: $0.1 < \Omega_m < 0.5$. Furthermore, we constrain the Hubble parameter to be uniformly in 4σ Hubble Space Telescope (HST) region: $0.4 < h < 1.0$. The resulting plots are produced with CosmoloGUI¹.

In this section we will list the cosmological observations used in our calculations: CMB, BAO and SNIa measurements, as well as some high-redshift observations, such as the GRB and LGF data. We have taken the total likelihood to be the products of the separate likelihoods (\mathcal{L}_i) of these cosmological probes. In other words, defining $\chi_{L,i}^2 = -2 \log \mathcal{L}_i$, we get:

$$\begin{aligned} \chi_{L,\text{total}}^2 &= \chi_{L,\text{CMB}}^2 + \chi_{L,\text{BAO}}^2 + \chi_{L,\text{SNIa}}^2 \\ &+ \chi_{L,\text{GRB}}^2 + \chi_{L,\text{LGF}}^2. \end{aligned} \quad (14)$$

If the likelihood function is Gaussian, χ_L^2 coincides with the usual definition of χ^2 up to an additive constant corresponding to the logarithm of the normalization factor of \mathcal{L} .

A. CMB Data

CMB measurement is sensitive to the distance to the decoupling epoch via the locations of peaks and troughs of the acoustic oscillations. Here we use the ‘‘WMAP distance information’’ obtained by the WMAP group [1], which includes the ‘‘shift parameter’’ R , the ‘‘acoustic scale’’ l_A , and the photon decoupling epoch z_* . R and l_A correspond to the ratio of angular diameter distance to the decoupling era over the Hubble horizon and the sound horizon at decoupling, respectively, given by:

$$R = \frac{\sqrt{\Omega_m H_0^2}}{c} \chi(z_*), \quad (15)$$

$$l_A = \frac{\pi \chi(z_*)}{\chi_s(z_*)}, \quad (16)$$

where $\chi(z_*)$ and $\chi_s(z_*)$ denote the comoving distance to z_* and the comoving sound horizon at z_* , respectively. The decoupling epoch z_* is given by [17]:

$$z_* = 1048[1 + 0.00124(\Omega_b h^2)^{-0.738}][1 + g_1(\Omega_m h^2)^{g_2}], \quad (17)$$

where

$$g_1 = \frac{0.0783(\Omega_b h^2)^{-0.238}}{1 + 39.5(\Omega_b h^2)^{0.763}}, \quad g_2 = \frac{0.560}{1 + 21.1(\Omega_b h^2)^{1.81}}. \quad (18)$$

¹ URL: <http://www.sarahbridle.net/cosmologui/>.

² In the revised version of WMAP5 paper [1], they also extend the baryon density $\Omega_b h^2$ into the WMAP distance information. But our calculations are not sensitive to $\Omega_b h^2$ and they also claim that this extension does not affect the constraints. Thus, we fix $\Omega_b h^2 = 0.022765$ to be the best fit value obtained by the WMAP group.

Table I. Inverse covariance matrix for the WMAP distance information l_A , R and z_* . The maximum likelihood values are $R = 1.710$, $l_A = 302.10$ and $z_* = 1090.04$, respectively.

	$l_A(z_*)$	$R(z_*)$	z_*
$l_A(z_*)$	1.800	27.968	-1.103
$R(z_*)$		5667.577	-92.263
z_*			2.923

We calculate the likelihood of the WMAP distance information as follows:

$$\chi^2 = (x_i^{\text{th}} - x_i^{\text{data}})(C^{-1})_{ij}(x_j^{\text{th}} - x_j^{\text{data}}), \quad (19)$$

where $x = (R, l_A, z_*)$ is the parameter vector and $(C^{-1})_{ij}$ is the inverse covariance matrix for the WMAP distance information shown in Table I.

B. BAO Data

The BAO information has been already detected in the current galaxy redshift survey. The BAO can directly measure not only the angular diameter distance, $D_A(z)$, but also the expansion rate of the universe, $H(z)$. But current BAO data are not accurate enough for extracting the information of $D_A(z)$ and $H(z)$ separately [18]. Therefore, one can only determine the following effective distance [19]:

$$D_v(z) \equiv \left[(1+z)^2 D_A^2(z) \frac{cz}{H(z)} \right]^{1/3}. \quad (20)$$

In this note we use the gaussian priors on the distance ratios $r_s(z_d)/D_v(z)$:

$$\begin{aligned} r_s(z_d)/D_v(z=0.20) &= 0.1980 \pm 0.0058, \\ r_s(z_d)/D_v(z=0.35) &= 0.1094 \pm 0.0033, \end{aligned} \quad (21)$$

with a correlation coefficient of 0.39, extracted from the SDSS and 2dFGRS surveys [20], where $r_s(z_d)$ is the comoving sound horizon size and z_d is the drag epoch at which baryons were released from photons given by [21]:

$$z_d = \frac{1291(\Omega_m h^2)^{0.251}}{1 + 0.659(\Omega_m h^2)^{0.828}} [1 + b_1(\Omega_b h^2)^{b_2}], \quad (22)$$

where

$$\begin{aligned} b_1 &= 0.313(\Omega_m h^2)^{-0.419} [1 + 0.607(\Omega_m h^2)^{0.674}], \\ b_2 &= 0.238(\Omega_m h^2)^{0.223}. \end{aligned} \quad (23)$$

C. SNIa Data

The SNIa data give the luminosity distance as a function of redshift

$$d_L = (1+z) \int_0^z \frac{cdz'}{H(z')}. \quad (24)$$

The supernovae data we use in this paper are the recently released Union compilation (307 sample) from the Supernova Cosmology project [2], which include the recent samples of SNIa from the SNLS and ESSENCE survey, as well as some older data sets, and span the redshift range $0 \lesssim z \lesssim 1.55$. In the calculation of the likelihood from SNIa we have marginalized over the nuisance parameter, the absolute magnitude M , as done in Ref.[22]:

$$\bar{\chi}^2 = A - \frac{B^2}{C} + \ln \left(\frac{C}{2\pi} \right), \quad (25)$$

where

$$\begin{aligned} A &= \sum_i \frac{(\mu^{\text{data}} - \mu^{\text{th}})^2}{\sigma_i^2}, \\ B &= \sum_i \frac{\mu^{\text{data}} - \mu^{\text{th}}}{\sigma_i^2}, \\ C &= \sum_i \frac{1}{\sigma_i^2}. \end{aligned} \quad (26)$$

D. GRB Data

GRBs can potentially be used to measure the luminosity distance out to higher redshift than SNIa. Recently, several empirical correlations between GRB observables were reported, and these findings have triggered intensive studies on the possibility of using GRBs as cosmological “standard” candles. However, due to the lack of low-redshift long GRBs data to calibrate these relations, in a cosmology-independent way, the parameters of the reported correlations are given, assuming an input cosmology, and obviously they depend on the same cosmological parameters that we would like to constrain. Thus, applying such relations to constrain cosmological parameters leads to biased results. In Ref.[23] the circular problem is naturally eliminated by marginalizing over the free parameters involved in the correlations; in addition, some results show that these correlations do not change significantly for a wide range of cosmological parameters [24]. Therefore, in this paper we use the 69 GRBs sample over a redshift range from $z = 0.17 - 6.60$ published in Ref.[25] but we keep in mind the issues related to the “circular problem” that are more extensively discussed in Ref.[23].

E. LGF Data

As we point out above, the linear growth factor will be suppressed in the modified gravity model. It will be helpful using the measurements of linear growth factor to constrain the modified gravity models. Therefore, in Table II we list linear growth factors data we use in our analysis: the linear growth rate $f \equiv \Omega_m^\gamma$ from galaxy power spectrum at low redshifts [26, 27, 28, 29, 30] and lyman- α growth factor measurement obtained with the

TABLE II. The currently available data for linear growth rates f we use in our analysis.

z	f	σ	Ref.
0.15	0.51	0.11	[26]
0.35	0.70	0.18	[27]
0.55	0.75	0.18	[28]
0.77	0.91	0.36	[29]
1.40	0.90	0.24	[30]
3.00	1.46	0.29	[31]

TABLE III. Constraints on the parameters α , Ω_m and γ . Here we have shown the mean values and errors from the current observations and the standard derivations from the future measurements.

	α	Ω_m	γ
CMB+BAO+SN	0.263 ± 0.175	0.276 ± 0.018	–
All Real Data	0.254 ± 0.153	0.277 ± 0.017	0.570 ± 0.205
Future	0.07	0.005	0.050

lyman- α power spectrum at $z = 3$ [31]. It is worth noting that the data points in Table II are obtained with assuming the Λ CDM model, thus, one should use these data very carefully, especially for the points obtained from Refs.[27, 28, 30]. The corresponding χ^2 is simply given by:

$$\chi^2 = \sum_i \frac{(f_i^{\text{th}} - f_i^{\text{data}})^2}{\sigma_i^2}. \quad (27)$$

IV. NUMERICAL RESULTS

In this section we present our main results of constraints on this phenomenological model from the current observational data, as shown in Table III.

In Fig.4 we illustrate the posterior distribution of α from the current data. Firstly, we neglect the high redshift probes. The result shows that the current observations yield a strong constraint on the parameter:

$$\alpha = 0.263 \pm 0.175 (1\sigma). \quad (28)$$

One can see that the pure Λ CDM model ($\alpha = 0$) still fits data very well at 2σ uncertainty, which is consistent with the current status of global fitting results [1, 32]. And the 95% upper limit is $\alpha < 0.686$, which implies that there is a significant tension between the flat DGP model ($\alpha = 1$) and the current observations, which is consistent with other works (e.g. Ref.[33, 34]). However, unlike other works [33], in our analysis we use the “WMAP distance information” which includes the “shift parameter” R , the “acoustic scale” l_A , and the photon

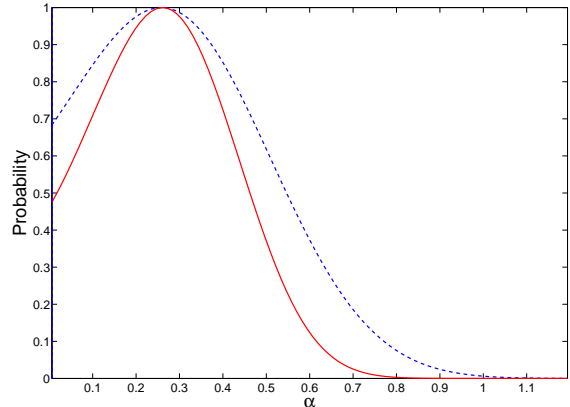


FIG. 4: One dimensional constraint on the parameter α from the different current data combinations: CMB+BAO+SN (blue dashed lines) and all real data (red solid lines).

decoupling epoch z_* , instead of R only, to constrain this phenomenological model. Recently, many results show that the “WMAP distance information” can give the similar constraints, when compared with the results from the full CMB power spectrum [35]. By contrast, R could not be an accurate substitute for the full CMB data and may in principle give some misleading results [36].

And then, we include some high redshift probes, such as GRB and LGF data sets. From Table III and Fig.4, we can find that the constraint on α becomes slightly tighter:

$$\alpha = 0.254 \pm 0.153 (1\sigma), \quad (29)$$

and $\alpha < 0.541$ at 2σ confidence level. As we have mentioned before, the effective equation of state of this phenomenological model will depart from the cosmological constant boundary at high redshifts. Therefore, these high redshift observations are helpful to improve the constraints on this phenomenological model.

These results (Eqs.(28-29)) are not surprising. From Fig.1 we find that the effective equation of state of the flat DGP model, $w_{\text{eff}} \approx -1 + \alpha/2 = -0.5$, will depart from the cosmological constant $w = -1$ at high-redshift universe significantly. But the current constraint on w is closed to $w = -1$ [1, 32], so we require the small value of α to match the current observations. There is a small difference that our result slightly favors a non-zero value of α , but not significantly, which needs more accurate measurements to verify it further.

In Fig.5 we plot the two dimensional constraint in the (Ω_m, α) panel. Ω_m and α are strongly anti-correlated. The reason of this degeneracy is that the constraint mainly comes from the luminosity and angular diameter distance information. From Eq.(3) and Eq.(4) we can see that when α is increased, the contribution of last α term to the expansion rate will become large, due to the positive $E(z)$. Consequently, Ω_m must be decreased corre-

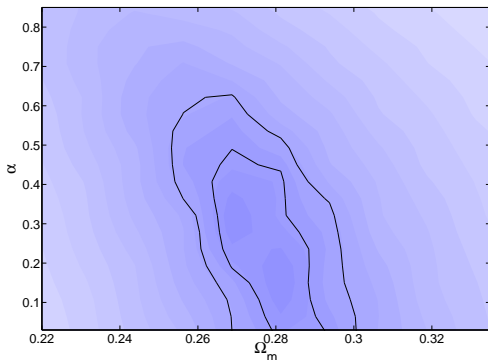


FIG. 5: 68% and 95% constraints in the (Ω_m, α) plane from the current observations.

spondingly in order to produce the same expansion rate. When combining those current observational data, the matter energy density has been constrained very stringent: $\Omega_m = 0.277 \pm 0.017$ (1σ), which is also consistent with the current status of global fitting results [1, 32]. Naturally, the constraint on α will also be improved, because of the tight constraint on the matter energy density.

Furthermore, we also investigate the limit on the growth index γ and obtain $\gamma = 0.570 \pm 0.205$ at 68% confidence level. Obviously, the growth index of the pure Λ CDM $\gamma = 6/11 \approx 0.545$ is consistent with this result. However, the theoretical value of growth index in the flat DGP model, $\gamma = 11/16 = 0.6875$, is disfavored.

V. FUTURE CONSTRAINTS

Since the present data clearly do not give very stringent constraint on the parameter α , it is worthwhile to discuss whether future data could determine α conclusively. For that purpose we have performed an analysis and chosen the fiducial model as the mean values of Table III obtained from the current constraints.

The projected satellite SNAP (Supernova / Acceleration Probe) would be a space based telescope with a one square degree field of view with 10^9 pixels. It aims to increase the discovery rate for SNIa to about 2000 per year in the redshift range $0.2 < z < 1.7$. In this paper we simulate about 2000 SNIa according to the forecast distribution of the SNAP [37]. For the error, we follow the Ref.[37] which takes the magnitude dispersion 0.15 and the systematic error $\sigma_{\text{sys}} = 0.02 \times z/1.7$. The whole error for each data is given by:

$$\sigma_{\text{mag}}(z_i) = \sqrt{\sigma_{\text{sys}}^2(z_i) + \frac{0.15^2}{n_i}}, \quad (30)$$

where n_i is the number of supernovae of the i 'th redshift bin. Furthermore, we add as an external data set a mock dataset of 400 GRBs, in the redshift range $0 < z < 6.4$

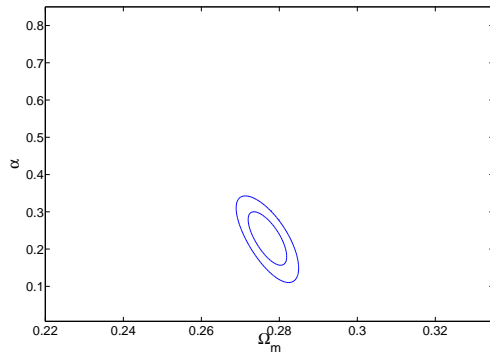


FIG. 6: 68% and 95% constraints in the (Ω_m, α) plane from the future measurements.

with an intrinsic dispersion in the distance modulus of $\sigma_\mu = 0.16$ and with a redshift distribution very similar to that of Figure 1 of Ref.[38].

For the linear growth factors data, we simulate the mock data from the fiducial model with the error bars reduced by a factor of two. This is probably reasonable given the larger amounts of galaxy power spectrum and Lyman- α forest power spectrum data that will become available soon as long with a better control of systematic errors in the next generated large scale structure survey. In addition we also assume a Gaussian prior on the matter energy density Ω_m as $\sigma = 0.007$, which is close to future Planck constraints [39].

From Table III it is clear that the future measurements with higher precision could improve the constraints dramatically. The standard deviation of α is reduced by a factor two. Assuming the mean value remains unchanged in the future, the non-zero value of α will be confirmed around 3σ confidence level by the future measurements. In addition we also illustrate the two dimensional contour of parameters Ω_m and α in Fig.6. Comparing with the contour in Fig.5, the allowed parameter region has been shrunk significantly. The future measurements could have enough ability to distinguish between the modified gravity model and the pure Λ CDM model.

VI. CONCLUSIONS

As an alternative approach to generate the late-time acceleration of the expansion of our universe, models of modifications of gravity have attracted a lot of interests in the phenomenological studies recently. In this note we investigate an interesting phenomenological model which interpolates between the pure Λ CDM model and the flat DGP braneworld model with an additional parameter α .

Firstly, we find that when α is less than zero, the growth function of density perturbation $\delta(a)$ will appear an apparent singularity. This is because the variable β will change the sign during the evolution of our universe.

And then the β term caused by the modified gravity model will be divergent at some redshift z_t .

From the current CMB, BAO and SNIa data, we obtain a tight constraint on the parameter $\alpha = 0.263 \pm 0.175$ (1σ), which implies that the flat DGP model ($\alpha = 1$) is incompatible with the current observations, while the pure Λ CDM model still fits the data very well. When adding the high-redshift GRB and LGF data, the constraint is more stringent $\alpha = 0.254 \pm 0.153$ (1σ), which

means that these high redshift observations are helpful to improve the constraints on this phenomenological model.

Finally, we simulate the future measurements with higher precisions to limit this phenomenological model. And we find that these accurate probes will be helpful to improve the constraints on the parameters of the model and could distinguish between the modified gravity model and the pure Λ CDM model.

-
- [1] E. Komatsu, *et al.*, arXiv:0803.0547.
[2] M. Kowalski *et al.*, arXiv:0804.4142.
[3] S. Weinberg, *Rev. Mod. Phys.* **61**, 1 (1989); I. Zlatev, L. M. Wang and P. J. Steinhardt, *Phys. Rev. Lett.* **82**, 896 (1999).
[4] S. M. Carroll, V. Duvvuri, M. Trodden, and M. S. Turner, *Phys. Rev. D* **70**, 043528 (2004); C. Schmid, J. P. Uzan and A. Riazuelo, *Phys. Rev. D* **71**, 083512 (2005).
[5] See e.g. V. Acquaviva, C. Baccigalupi and F. Perrotta, *Phys. Rev. D* **70**, 023515 (2004); P. Zhang, *Phys. Rev. D* **73**, 123504 (2006); Y. S. Song, H. Peiris and W. Hu, *Phys. Rev. D* **76**, 063517 (2007); E. Bertschinger and P. Zukin, *Phys. Rev. D* **78**, 024015 (2008); and references therein.
[6] S. F. Daniel, R. R. Caldwell, A. Cooray and A. Melchiorri, *Phys. Rev. D* **77**, 103513 (2008); S. F. Daniel, R. R. Caldwell, A. Cooray, P. Serra and A. Melchiorri, arXiv:0901.0919.
[7] G. R. Dvali, G. Gabadadze and M. Porrati, *Phys. Lett. B* **485**, 208 (2000).
[8] C. Deffayet, *Phys. Lett. B* **502**, 199 (2001).
[9] A. Lue, *Phys. Rept.* **423**, 1 (2006).
[10] C. Deffayet, *Int. J. Mod. Phys. D* **16** (2008) 2023; R. Durrer and R. Maartens, arXiv:0811.4132; and references therein.
[11] G. Dvali and M. S. Turner, arXiv:astro-ph/0301510.
[12] K. Koyama and R. Maartens, *JCAP* **0601**, 16 (2006).
[13] K. Koyama, *JCAP* **0603**, 17 (2006).
[14] E. V. Linder, *Phys. Rev. D* **72**, 043529 (2005); D. Huterer and E. V. Linder, *Phys. Rev. D* **75**, 023519 (2007); D. Polarski, arXiv:astro-ph/0605532; S. A. Thomas, F. B. Abdalla and J. Weller, arXiv:0810.4863.
[15] P. J. E. Peebles, *Large-Scale Structure of the Universe*, Princeton Univ. Press, 1980; P. J. E. Peebles, *Astrophys. J.* **284**, 439 (1984); O. Lahav, P. B. Lilje, J. R. Primack and M. J. Rees, *Mon. Not. R. Astron. Soc.* **251**, 128 (1991).
[16] E. V. Linder and R. N. Cahn, *Astropart. Phys.* **28**, 481 (2007).
[17] W. Hu and N. Sugiyama, *Astrophys. J.* **471**, 542 (1996).
[18] T. Okumura, T. Matsubara, D. J. Eisenstein, I. Kayo, C. Hikage, A. S. Szalay and D. P. Schneider, *Astrophys. J.* **677**, 889 (2008).
[19] D. J. Eisenstein *et al.* *Astrophys. J.* **633**, 560 (2005).
[20] W. J. Percival, *et al.*, *Mon. Not. Roy. Astron. Soc.* **381**, 1053 (2007).
[21] D. Eisenstein and W. Hu, *Astrophys. J.* **496**, 605 (1998).
[22] E. Di Pietro and J. F. Claeskens, *Mon. Not. Roy. Astron. Soc.* **341**, 1299 (2003).
[23] H. Li, J. Q. Xia, J. Liu, G. B. Zhao, Z. H. Fan and X. Zhang, *Astrophys. J.* **680**, 92 (2008).
[24] C. Firmani, V. Avila-Reese, G. Ghisellini and G. Ghirlanda, *Rev. Mex. Astron. Astrofis.* **43**, 203 (2007).
[25] B. E. Schaefer, *Astrophys. J.* **660**, 16 (2007).
[26] E. Hawkins *et al.*, *Mon. Not. Roy. Astron. Soc.* **346**, 78 (2003); L. Verde *et al.*, *Mon. Not. Roy. Astron. Soc.* **335**, 432 (2002).
[27] M. Tegmark *et al.*, *Phys. Rev. D* **74**, 123507 (2006).
[28] N. P. Ross *et al.*, arXiv:astro-ph/0612400.
[29] L. Guzzo *et al.*, *Nature* **451**, 541 (2008).
[30] J. da Angela *et al.*, arXiv:astro-ph/0612401.
[31] P. McDonald *et al.* *Astrophys. J.* **635**, 761 (2005).
[32] J. Q. Xia, H. Li, G. B. Zhao and X. Zhang, *Phys. Rev. D* **78**, 083524 (2008).
[33] M. Fairbairn and A. Goobar, *Phys. Lett. B* **642**, 432 (2006); Z. K. Guo, Z. H. Zhu, J. S. Alcaniz and Y. Z. Zhang, *Astrophys. J.* **646**, 1 (2006); S. Rydbeck, M. Fairbairn and A. Goobar, *JCAP* **0705**, 003 (2007); T. M. Davis *et al.*, *Astrophys. J.* **666**, 716 (2007); M. S. Movahed, M. Farhang and S. Rahvar, *Int. J. Theor. Phys.* **48**, 1203 (2009).
[34] Y. S. Song, *Phys. Rev. D* **71**, 024026 (2005); Y. S. Song, I. Sawicki and W. Hu, *Phys. Rev. D* **75**, 064003 (2007); W. Fang, S. Wang, W. Hu, Z. Haiman, L. Hui and M. May, *Phys. Rev. D* **78**, 103509 (2008); Z. H. Zhu and M. Sereno, arXiv:0804.2917; S. A. Thomas, F. B. Abdalla and J. Weller, arXiv:0810.4863; and references therein.
[35] P. S. Corasaniti and A. Melchiorri, *Phys. Rev. D* **77**, 103507 (2008); H. Li, J. Q. Xia, G. B. Zhao, Z. H. Fan and X. Zhang, *Astrophys. J.* **683**, L1 (2008).
[36] O. Elgaroy and T. Multamaki, *Astron. Astrophys.* **471**, 65 (2007).
[37] A. G. Kim, E. V. Linder, R. Miquel and N. Mostek, *Mon. Not. Roy. Astron. Soc.* **347**, 909 (2004).
[38] D. Hooper and S. Dodelson, *Astropart. Phys.* **27**, 113 (2007).
[39] Planck Collaboration, arXiv:astro-ph/0604069.